Articles

Thermolysis of Surface-Attached 1,3-Diphenylpropane: Radical Chain Induced Decomposition under Conditions of Restricted Diffusion

A. C. Buchanan, III,* and Cheryl A. Biggs

Chemistry Division, Oak Ridge National Laboratory, P.O. Box 2008, Oak Ridge, Tennessee 37831-6197

Received August 16, 1988

Surface-immobilized 1,3-diphenylpropane (~~$Ph(CH_2)_3Ph$, or ~~DPP) has been prepared by the condensation of *p*-(3-phenylpropyl)phenol with the surface hydroxyl groups of an amorphous, fumed silica. Thermolysis studies of the covalently attached ~~DPP have been conducted to explore the effects of restricted radical and substrate diffusion on a free-radical chain induced decomposition reaction, which has been reported to underlie the thermal reactivity of fluid-phase DPP at ≤400 °C. Thermolysis of ~~DPP has been studied at 345–400 °C as a function of ~~DPP conversion (0.3–23%) and initial surface coverage (0.132–0.586 mmol g^{-1}; 0.43–1.97 DPP molecules nm^{-2}). Decomposition of surface-immobilized ~~DPP occurs readily in this temperature range by parallel free-radical chain pathways, whose rates are quite sensitive to surface coverage, producing ~~$PhCH_3$ + ~~$PhCH{=}CH_2$ and ~~$PhCH_3$ + $PhCH{=}CH_2$ as the major product pairs. An unusual regiospecific hydrogen transfer process is observed that favors formation of ~~$PhCH_2CH_2\dot{C}HPh$ over ~~$Ph\dot{C}HCH_2CH_2Ph$ as the proximity of ~~DPP molecules and hydrogen abstracting radicals on the surface decreases. This phenomenon results in regioselective cracking of ~~DPP favoring the ~~$PhCH_3$ + $PhCH{=}CH_2$ product pair. Implications are discussed for the thermal degradation of related structural features in a diffusionally restricted, macromolecular network such as occurs in coal.

Introduction

Thermolysis studies of organic compounds that serve as models for structural features present in coal have provided valuable insights into the kinetic and mechanistic behavior of many key structural elements.[1-9] The resulting knowledge has enhanced current understanding of the thermal reactivity of coal, which underpins many technologically important processes such as coal pyrolysis and hydropyrolysis[2b,10,11b,c,12] and liquefaction.[2c,11d,e,12,13] Our research interest has turned toward modeling the constraints on free-radical reactions that might be imposed in coal as a consequence of its cross-linked macromolecular structure.[11a,14,15] This complicating feature could significantly perturb the extrapolation of simple model compound behavior in fluid phases to that of similar features in coal itself. In order to study this restricted-mobility phenomenon at temperatures relevant to coal thermolysis, which begins to occur at 350–400 °C, we have developed procedures that allow the investigation of the thermal reactivity of substituted aromatic model compounds that are covalently anchored to an inert silica surface.[16] The ≡$SiOC_{aryl}$ linkage employed is thermally robust in the temperature range of interest.

We recently showed that, as in the liquid and vapor phases, surface-immobilized biphenyl (denoted ~~PhPh) and diphenylmethane (~~$PhCH_2Ph$) do not react after several hours of heating in vacuum at 400 °C.[16] This indicated that the remaining underivatized surface hydroxyl groups on the high purity, fumed silica do not catalyze any new reaction pathways. Moreover, a detailed study of the thermolysis of surface-immobilized bibenzyl (~~$PhCH_2CH_2Ph$) showed that the rate of unimolecular C–C homolysis is similar to that in fluid phases and, hence, is also not perturbed by the mode of surface attachment. For example, at 375 °C, the first-order rate constants for the initial homolysis of gaseous, liquid (in tetralin), and surface-immobilized bibenzyl are 2.2, 1.1, and 1.2×10^{-6} s^{-1}, respectively.[16a] However, we found that restricted radical and substrate mobility can cause dramatic changes in free-radical reaction pathways compared with those in fluid phases. In particular, complex free-radical chain

* Research sponsored by the Division of Chemical Sciences/Office of Basic Energy Sciences, U.S. Department of Energy under contract DE-AC05-840R21400 with the Martin Marietta Energy Systems, Inc.

(1) Stein, S. E. *ACS Symp. Ser.* **1981**, No. *169*, 97.
(2) (a) Stein, S. E. *Chemistry of Coal Conversion*; Schlosberg, R. H., Ed.; Plenum Press: New York, 1985; Chapter 2. (b) Solomon, P. R.; Hamblen, D. G. *Ibid.* Chapter 5. (c) Stock, L. M. *Ibid.* Chapter 6.
(3) (a) McMillen, D. F.; Malhotra, R.; Chang, S.-J.; Ogier, W. C.; Nigenda, S. E.; Fleming, R. H. *Fuel* **1987**, *66*, 1611. (b) McMillen, D. F.; Ogier, W. C.; Ross, D. S. *J. Org. Chem.* **1981**, *46*, 3322.
(4) Franz, J. A.; Camaioni, D. M.; Beishline, R. R.; Dalling, D. K. *J. Org. Chem.* **1984**, *49*, 3563.
(5) Bockrath, B.; Bittner, E.; McGrew, J. *J. Am. Chem. Soc.* **1984**, *106*, 135.
(6) Hung, M.-M.; Stock, L. M. *Fuel* **1982**, *61*, 1161.
(7) (a) Benjamin, B. M.; Raaen, V. F.; Maupin, P. H.; Brown, L. L.; Collins, C. J. *Fuel* **1978**, *57*, 269. (b) Collins, C. J.; Raaen, V. F.; Benjamin, B. M.; Maupin, P. H.; Roark, W. H. *J. Am. Chem. Soc.* **1979**, *101*, 5009.
(8) (a) Poutsma, M. L. *Fuel* **1980**, *59*, 1980. (b) Poutsma, M. L.; Dyer, C. W. *J. Org. Chem.* **1982**, *47*, 3367.
(9) Squire, K. R.; Solomon, P. R.; Carangelo, R. M.; DiTaranto, M. B. *Fuel* **1986**, *65*, 833.
(10) Gavalas, G. R. *Coal Pyrolysis*; Elsevier: Amsterdam, 1982.
(11) (a) Wender, I.; Heredy, L. A.; Neuworth, M. B.; Dryden, I. G. C. *Chemistry of Coal Utilization*; Elliot, M. A., Ed.; Wiley-Interscience: New York, 1981; Suppl. Vol. 2, Chapter 8. (b) Howard, J. B. *Ibid.* Chapter 12. (c) Seglin, L.; Bresler, S. A. *Ibid.* Chapter 13. (d) Gorin, E. *Ibid.* Chapter 27. (e) Alpert, S. B.; Wolk, R. H. *Ibid.* Chapter 28.
(12) Berkowitz, N. *The Chemistry of Coal, Coal Science and Technology*; Elsevier: Amsterdam, 1985; Vol. 11.
(13) Whitehurst, D. D.; Mitchell, T. O.; Farcasiu, M. *Coal Liquefaction*; Academic Press: New York, 1980.
(14) Davidson, R. M. In *Coal Science*; Gorbaty, M. L., Larsen, J. W., Wender, I., Eds.; Academic Press: New York, 1982; Vol. 1.
(15) Green, T.; Kovac, J.; Brenner, D.; Larsen, J. W. In *Coal Structure*; Meyers, R. A., Ed.; Academic Press: New York, 1982; Chapter 6.
(16) (a) Buchanan, A. C., III; Dunstan, T. D. J.; Douglas, E. C.; Poutsma, M. L. *J. Am. Chem. Soc.* **1986**, *108*, 7703. (b) Poutsma, M. L.; Douglas, E. C.; Leach, J. E. *J. Am. Chem. Soc.* **1984**, *106*, 1136.

0022-3263/89/1954-0517$01.50/0

pathways became major thermal decay routes on the surface leading to an actual acceleration in the total rate of decomposition for the immobilized bibenzyl as well as a vastly different product mixture. These enhanced radical chain pathways on the surface resulted in substantial isomerization [to form ~~PhCH(Ph)CH_3], cyclization–dehydrogenation (to form ~~dihydrophenanthrene and ~~phenanthrene), and hydrogenolysis (to form ~~PhH + PhC_2H_5 and ~~PhC_2H_5 + PhH) of bibenzyl groups.

In this paper we examine the influence of surface immobilization on the thermolysis of 1,3-diphenylpropane (DPP),[17] whose fluid-phase behavior has been extensively studied.[7,18-21] Thermolysis of liquid DPP occurs at a faster rate than that of bibenzyl despite the fact that DPP contains no bond that is as thermally labile as the central C–C bond in bibenzyl.[22] It is now well documented through mechanistic studies that the facile thermal cracking of DPP at 350–400 °C (eq 1) occurs via an induced decomposition reaction in a long chain free-radical process rather than by rate-controlling C–C homolysis.[18,19a] Kinetic orders of approximately 3/2 (1.59,[18] 1.55[19a]), activation energies of ca. 52 kcal/mol (52.3,[18] 51.4[19a]), rate acceleration by addition of free-radical initiators,[19,21] results of deuterium labeling experiments,[18] and thermochemical analysis[18] were all consistent with the mechanistic scheme shown in eq 2–6, where eq 4 and 5 are the chain propagation steps and the simplified steady-state rate expression, rate = $(k_2/k_6)^{1/2}k_4[1]^{3/2}$, results from the fact that $k_5 \gg k_4[1]$.

$$Ph(CH_2)_3Ph \rightarrow PhCH_2^{\bullet} + PhCH_2CH_2^{\bullet} \quad (2)$$
1

$$PhCH_2CH_2^{\bullet} + 1 \rightarrow PhCH_2CH_3 + \overset{\bullet}{P}hCHCH_2CH_2Ph \quad (3)$$
2

$$PhCH_2^{\bullet} + 1 \rightarrow PhCH_3 + 2 \quad (4)$$

$$2 \rightarrow PhCH{=}CH_2 + PhCH_2^{\bullet} \quad (5)$$

$$2PhCH_2^{\bullet} \rightarrow PhCH_2CH_2Ph \quad (6)$$

These fluid-phase studies suggest that three-carbon bridges (and probably longer[6,18]) between aromatic moieties in coal are likely to cleave under mild thermal conditions as a result of similar induced decomposition pathways that involve β-scission of radicals such as **2**. However, it is not clear to what extent these processes may be perturbed in a macromolecular framework such as occurs in coal. Hence, we have prepared surface-immobilized 1,3-diphenylpropane (~~DPP) as a model and studied its reactivity at 345–400 °C as a function of conversion and surface coverage to examine the influence of restricted diffusion on the radical chain induced decomposition process.

Results

Preparation of Surface-Attached 1,3-Diphenylpropane (~~DPP, or 3). Two batches of ~~DPP were prepared at saturation coverage as shown in eq 7 by the condensation of excess p-$HOC_6H_4(CH_2)_3C_6H_5$ with the surface hydroxyls of a high-purity fumed silica.

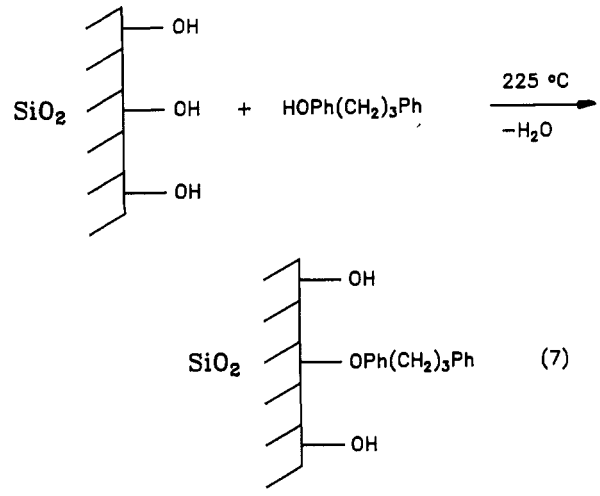

(7)

Analysis of the surface coverage, by GC of parent phenol liberated from a base hydrolysis procedure, gave consistent coverages of 0.586 (batch A) and 0.566 (batch B) mmol of ~~DPP/g of derivatized silica with purities of 99.7 and 99.9%, respectively. The average coverage of 0.576 mmol/g corresponds to ca. 1.97 DPP molecules/nm^2 of surface area, indicating that approximately 40–50% of the surface hydroxyls have been derivatized. The efficiency of packing of substituted benzenes attached to the amorphous silica surface was considered previously by using crystalline silica surfaces as models.[16] The present level of "saturation" surface coverage for ~~DPP, which is slightly larger than that for surface-attached bibenzyl, is consistent with a "liquid-like" monolayer with steric constraints prohibiting substantially higher coverages.

Two batches with approximately one-fourth the saturation surface coverage were prepared in a similar fashion, by limiting the initial phenol to surface hydroxyl ratio. These two batches were analyzed to have surface coverages of 0.142 and 0.132 mmol g^{-1} (ca. 0.43 DPP molecule nm^{-2}) with purities of 99.8%.

Thermolysis of ~~DPP. Thermolyses were performed in sealed evacuated Pyrex tubes with a T-shaped configuration such that volatile products could be collected in a cold trap as they formed. The volatile products in the trap were analyzed by GC and GC–MS. In a separate procedure, surface-attached products were liberated as phenols following digestion of the silica in base, silylated to the corresponding trimethylsilyl ethers, and analyzed as above.

Thermolysis of ~~DPP at saturation (or high) coverages was studied at 345–400 °C from 1.5 to 23% conversion, and quantitative data for the products described below are presented in Table I. Phenolic products described below were obtained after the digestion procedure and correspond to the surface-attached products indicated in parentheses and also shown in Table I. At low conversions (<3%), four major products are formed in nearly equal amounts: toluene ($PhCH_3$, **4**), p-hydroxystyrene (~~$PhCH{=}CH_2$, **5**), p-cresol (~~$PhCH_3$, **6**), and styrene ($PhCH{=}CH_2$, **7**). Other products detected at trace levels (each <0.07 mol %) are ethylbenzene (PhC_2H_5, **8**), p-ethylphenol (~~PhC_2H_5, **9**), and 1,2-diphenylethane ($PhCH_2CH_2Ph$, **10**). At higher conversions, additional products are detected in small amounts: 1,3-bis(p-hydroxyphenyl)propane (~~$Ph(CH_2)_3Ph$~~, **11**) and a mixture of isomeric diphenols of composition $C_{23}H_{22}(OH)_2$ (labeled ~~$C_{23}H_{22}$~~, **12**). Two of the isomeric di-

(17) For a preliminary communication of the present work, see: Buchanan, A. C., III; Biggs, C. A. *Prepr. Pap.—Am. Chem. Soc., Div. Fuel Chem.* **1987**, *32*(3), 175.
(18) Poutsma, M. L.; Dyer, C. W. *J. Org. Chem.* **1982**, *47*, 4903.
(19) (a) Gilbert, K. E.; Gajewski, J. J. *J. Org. Chem.* **1982**, *47*, 4899. (b) Gilbert, K. E. *J. Org. Chem.* **1984**, *49*, 6.
(20) Sweeting, J. W.; Wilshire, J. F. K. *Aust. J. Chem.* **1962**, *15*, 89.
(21) (a) King, H.-H.; Stock, L. M. *Fuel* **1982**, *61*, 1172; (b) *Ibid.* **1984**, *63*, 810.
(22) The bond dissociation energies, $D°$, for $PhCH_2$–CH_2Ph and $PhCH_2$–CH_2CH_2Ph are about 62 and 72 kcal mol^{-1}, respectively, predicting a rate depression of $>10^3$ for bond homolysis at 400 °C in going from the dimethylene to the trimethylene bridge.[18]

Table I. Products from Thermolysis of ~~Ph(CH$_2$)$_3$Ph at High Coverage

coverage (mmol/g)	0.566	0.566	0.566	0.566	0.566	0.566	0.566	0.566	0.566	0.566	0.586	0.586	0.586	0.586	0.586
temperature (°C)	345	345	375	375	375	375	375	375	400	400	375	375	375	375	375
time (min)[a]	20	30	10	10	40	60	150	240	5	10	10	20	40	60	150
charge (mmol)	0.198	0.187	0.206	0.194	0.186	0.202	0.204	0.193	0.195	0.183	0.180	0.165	0.187	0.176	0.172
~~Ph(CH$_2$)$_3$Ph (mol, rel)[b]															
charged	100	100	100	100	100	100	100	100	100	100	100	100	100	100	100
unreacted + evolved[c]	93.3	95.1	98.6	98.8	83.8	92.1	86.2	74.3	95.2	93.6	97.7	95.2	92.3	90.6	78.4
consumed	6.7	4.9	1.4	1.2	16.2	7.9	13.8	25.7	4.8	6.4	2.3	4.8	7.7	9.4	21.6
total products															
equiv, rel[d]	1.5	1.9	2.2	2.6	5.6	7.9	11.3	19.5	3.2	4.8	3.1	4.8	8.9	10.2	23.1
mol, rel	3.0	3.9	4.5	5.2	11.0	15.5	21.8	37.9	6.5	9.5	6.2	9.6	17.2	19.6	43.5
product distribution[e] (mol, rel)															
PhCH$_3$ (4)	0.74	0.99	1.07	1.28	2.72	3.85	5.11	8.13	1.52	2.30	1.58	2.42	4.14	4.60	9.13
~~PhCH=CH$_2$ (5)	0.76	0.97	1.17	1.29	2.54	3.14	4.20	6.45	1.68	2.24	1.51	2.23	3.58	4.01	6.86
~~PhCH$_3$ (6)	0.75	0.92	1.14	1.35	2.68	3.82	5.93	10.8	1.70	2.42	1.47	2.29	4.30	5.11	12.4
PhCH=CH$_2$ (7)	0.75	0.97	1.08	1.30	2.87	4.40	5.95	11.3	1.53	2.42	1.58	2.50	4.72	5.32	12.9
~~PhCH$_2$CH$_3$ (9)	*h*	*h*	*h*	0.01	0.01	0.020	0.092	0.23	0.012	0.026	0.012	0.014	0.031	0.046	0.21
~~Ph(CH$_2$)$_3$Ph~~ (11)	*h*	*h*	0.01	0.016	0.088	0.15	0.30	0.63	0.024	0.074	0.04	0.08	0.24	0.30	1.21
~~(C$_{23}$H$_{22}$)~~ (12)	*h*	*h*	*h*	*h*	0.054	0.12	0.26	0.32	*h*	0.038	*h*	0.02	0.17	0.24	0.77
product relationships															
PhCH=CH$_2$/PhCH$_3$	1.01	0.98	1.01	1.02	1.06	1.14	1.16	1.39	1.01	1.05	1.00	1.03	1.14	1.16	1.41
(free C$_7$)/(∑~~C$_8$)[f]	0.97	1.02	0.91	0.97	1.01	1.12	1.05	1.07	0.89	0.97	1.01	1.03	1.03	1.00	1.01
(free C$_8$)/(∑~~C$_7$)[g]	1.00	1.05	0.94	0.95	1.04	1.11	0.96	0.99	0.89	0.97	1.05	1.05	1.04	0.98	0.95

[a] Heat-up time is 1 min. [b] One hundred relative moles basis. [c] HOC$_6$H$_4$(CH$_2$)$_3$Ph recovered after reaction from residue analysis plus that evolved into cold trap. [d] C$_{15}$ equivalent basis. [e] Occasionally detect PhCH$_2$CH$_3$ (8) and Ph(CH$_2$)$_2$Ph (10) as products at trace levels (see text). [f] Defined as (4)/[(5) + (9) + (11) + (12)]. [g] Defined as (7)/[(6) + (11)]. [h] Below detection limit.

phenols (comprising ca. 40% of the isomeric mix) correspond to the two possible doubly attached 1,3,5-triphenylpentane isomers, ~~PhCH(CH$_2$CH$_2$Ph~~)CH$_2$CH$_2$Ph and ~~PhCH$_2$CH$_2$CH(CH$_2$CH$_2$Ph~~)Ph based on GC–MS and comparison of the trimethylsilyl ether derivatives with the corresponding products produced from a recent study of the thermolysis of fluid-phase *p*-(CH$_3$)$_3$SiOC$_6$H$_4$(CH$_2$)$_3$Ph.[23] The other four compounds (comprising 60% of the isomeric mix) have been identified as diphenols and have the same molecular weight and somewhat similar fragmentation patterns in the GC–MS as the two triphenylpentane isomers described above, but have not yet been identified.

Thermolyses of ~~DPP at lower coverages were performed at 345–375 °C with ~~DPP conversions of 0.28–3.9%. No new products were detected in these experiments, and quantitative data for product formation are given in Table II. The ~~DPP thermolysis rate was slightly accelerated by the addition of benzyl phenyl ether, PhCH$_2$OPh (BPE), as a free-radical initiator.[19] Reactions were run with the 0.132 mmol g^{-1} batch of ~~DPP for 40 min at 345 °C in the presence of 7 and 20 mol % initial amounts of BPE (the actual effective concentration of the initiator is not known since it rapidly distills out of the heated zone into the cold trap). The ~~DPP conversion increases with increasing initial concentration of BPE from 0.7% with no added BPE to 1.1 and 1.5% with 7 and 20 mol % initially of BPE.

During the thermolysis of both high- and low-coverage batches, some ~~DPP is detached from the surface as the phenol, evolved into the cold trap, and subsequently analyzed as unreacted starting material. This process, which was observed previously for other ~~Ph(CH$_2$)$_n$Ph,[16] is attributed to the condensation of ~~DPP with adjacent underivatized surface hydroxyls to generate parent phenol (HODPP) and a siloxane linkage in a process analogous to the thermally induced dehydroxylation of silica itself.[24] For thermolyses run with low-coverage batches, only small amounts of the parent phenol (2–7 mol %) were evolved into the cold trap, while the amounts were somewhat larger (6–19 mol %) for thermolyses run with the high-coverage batches. The ≡SiOC$_{aryl}$ covalent linkage is again found to be stable enough to keep most of the organic moieties on the surface for the reaction periods and temperatures employed in this study.

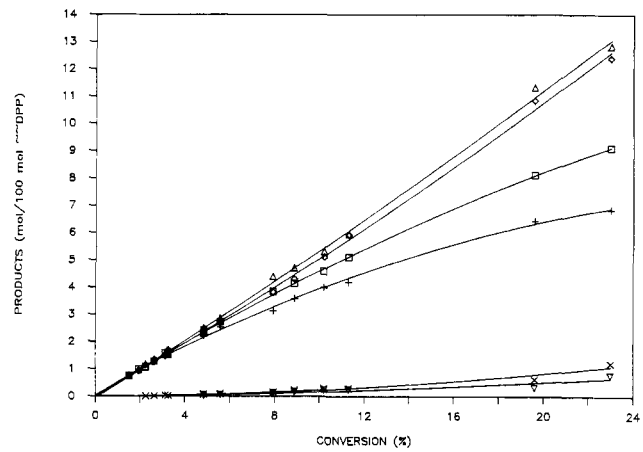

Figure 1. Product selectivities as a function of conversion level for thermolysis of surface-attached 1,3-diphenylpropane (~~DPP, 3) at 345–400 °C and saturation coverage: □, PhCH$_3$; +, ~~PhCH=CH$_2$; ◇, ~~PhCH$_3$; △, PhCH=CH$_2$; ×, ~~Ph(CH$_2$)$_3$Ph~~, ▽, ~~C$_{23}$H$_{22}$~~.

Discussion

Reaction Stoichiometry and Selectivity. Product yields for the thermolysis of ~~DPP at high coverage are given in Table I and are plotted as a function of conversion in Figure 1. The figure contains data obtained from both high-coverage batches at all temperatures studied (primarily at 375 °C) for the four main primary products and the two principal secondary products. The data at 345 and 400 °C were confined to <5% ~~DPP conversion, and no effect of temperature on product selectivities was discerned. We use as the measure of ~~DPP conversion the values for total products formed on a C$_{15}$ equivalent basis (Table I, row 8). Ideally these values should equal the calculated values for consumption of ~~DPP (row 7), which they generally do within experimental error. However, the value for "~~DPP consumed" suffers in accu-

(23) Britt, P. F., unpublished data.
(24) Iler, R. K. *The Chemistry of Silica*; Wiley: New York, 1979.

Table II. Products from Thermolysis of ~~Ph(CH$_2$)$_3$Ph at Low Coverage

coverage (mmol/g)	0.142	0.142	0.142	0.142	0.142	0.142	0.132	0.132	0.132	0.132	0.132	0.132	0.132
temperature (°C)	375	375	375	375	375	375	345	345	345	345	345	375	375
time (min)[a]	20	60	150	150	240	240	5	10	20	20	40	150	480
charge (mmol)	0.0886	0.0686	0.0687	0.0696	0.0690	0.0709	0.0690	0.0829	0.0793	0.0960	0.0826	0.0857	0.0840	0.0768	0.0857
~~Ph(CH$_2$)$_3$Ph (mol, rel)[a]													
charged	100	100	100	100	100	100	100	100	100	100	100	100	100	100	100
unreacted + evolved[a]	97.1	97.4	98.6	97.5	98.4	98.4	98.4	98.7	100.9	103.7	100.9	100.3	96.3	91.5	94.7
consumed	2.9	2.6	1.4	2.5	1.6	1.6	1.6	1.3	–0.9	–3.7	–0.9	–0.3	3.7	8.5	5.3
total products															
equiv, rel[a]	1.5	1.5	1.6	2.2	2.2	2.5	3.1	0.3	0.4	0.5	0.8	0.7	1.5	2.6	3.9
mol, rel	3.0	3.1	3.2	4.4	4.4	5.1	6.2	0.6	0.7	1.0	1.5	1.4	3.0	5.2	7.8
product distribution[b] (mol, rel)															
PhCH$_3$ (4)	0.66	0.68	0.72	0.96	1.01	1.12	1.47	0.13	0.17	0.23	0.36	0.34	0.71	1.19	1.67
~~PhCH=CH$_2$ (5)	0.79	0.79	0.78	1.10	1.07	1.26	1.40	0.14	0.18	0.27	0.36	0.37	0.67	1.21	1.75
~~PhCH$_3$ (6)	0.81	0.85	0.85	1.20	1.19	1.38	1.61	0.14	0.19	0.27	0.37	0.36	0.78	1.36	2.21
PhCH=CH$_2$ (7)	0.73	0.76	0.81	1.12	1.17	1.30	1.71	0.14	0.19	0.26	0.41	0.37	0.82	1.39	2.08
~~PhCH$_2$CH$_3$ (9)	*e*	*e*	*e*	*e*	*e*	0.01	0.02	*e*	*e*	*e*	*e*	*e*	*e*	0.01	0.12
product relationships															
PhCH=CH$_2$/PhCH$_3$	1.11	1.12	1.13	1.17	1.16	1.16	1.16	1.08	1.12	1.13	1.14	1.09	1.15	1.17	1.25
(free C$_7$)/($\sum$~~C$_8$)[c]	0.84	0.86	0.92	0.87	0.94	0.88	1.04	0.93	0.94	0.85	1.00	0.92	1.06	0.98	0.89
(free C$_8$)/($\sum$~~C$_7$)[d]	0.90	0.89	0.95	0.93	0.98	0.94	1.06	1.00	1.00	0.96	1.11	1.03	1.05	1.02	0.94

[a] Same meaning as in Table I. [b] Occasionally detect PhCH$_2$CH$_3$ and Ph(CH$_2$)$_2$Ph as products at trace levels (see text). [c] Defined as (4)/[(5) + (9)]. [d] Defined as (7)/(6). [e] Below detection limit.

racy from being the small difference between two large numbers (one of which is a sum of two measured values), and hence, we find the total product equivalent basis to be a more accurate measure of ~~DPP conversion.

At low conversions (<3%), ~~DPP cracks to form four major products in nearly equal yields as shown in eq 8 and

$$\sim\sim\mathrm{Ph(CH_2)_3Ph} \rightarrow \underset{\mathbf{4}}{\mathrm{PhCH_3}} + \underset{\mathbf{5}}{\sim\sim\mathrm{PhCH{=}CH_2}} + \underset{\mathbf{6}}{\sim\sim\mathrm{PhCH_3}} + \underset{\mathbf{7}}{\mathrm{PhCH{=}CH_2}} \quad (8)$$

Figure 1. This reaction is analogous to the thermal cracking reaction at low conversion for fluid-phase DPP (eq 1), with the additional product pair resulting from the fact that the two ends of the DPP molecule are no longer equivalent upon surface attachment. The initial rate of ~~DPP decomposition at these low conversions, which is slightly overestimated (see below), is 15–20% h^{-1} at 375 °C for the two batches based on a 2.2–3.1% conversion after a 9-min reaction period. Although the rate of ~~ DPP thermolysis will be discussed in more detail below, this initial rate is comparable to the 9–18% h^{-1} rate calculated for liquid-phase DPP at 375 °C based on published Arrhenius parameters.[18,19a] In addition, we found that the reaction rate for ~~DPP thermolysis could be accelerated by the addition of small amounts of PhCH$_2$OPh as a radical initiator as observed previously for liquid DPP.[19a] The similarities in product compositions, reaction rates, and effects of added free-radical initiators strongly suggest that ~~DPP is decomposing by a similar free-radical chain pathway as in the case of fluid-phase DPP.

A reaction scheme for the thermolysis of surface-immobilized DPP, analogous to the one determined for fluid-phase DPP, is shown in eq 9–14. The brackets in eq 10 and 11 are used as simplification to indicate that two equations may be written in each case, one with a surface-attached species and one with a vapor-phase species.

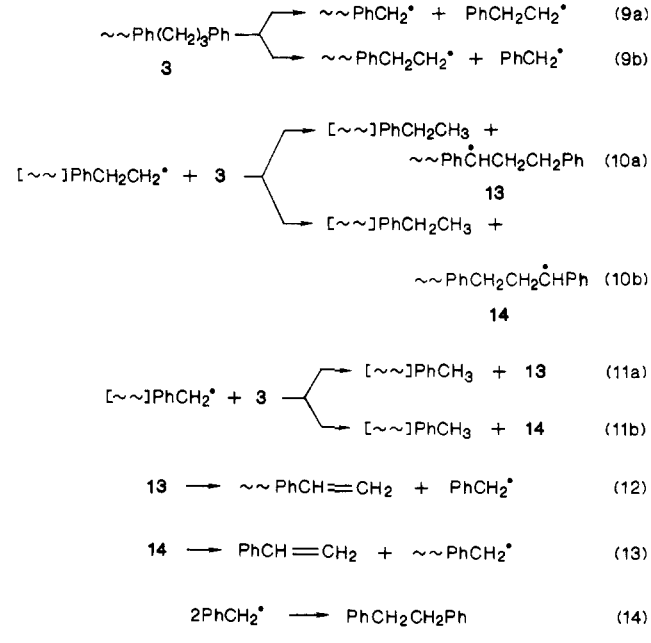

As in the case of fluid-phase DPP, in the absence of added radical sources, the reaction is initiated by radicals formed from a very small amount of homolysis (eq 9). The chain propagation steps (eq 11–13) are analogous to those for the free DPP (eq 4 and 5) except that on the surface

two chemically distinct benzylic radicals (**13** and **14**) are produced by hydrogen abstraction, which undergo subsequent β-scission to form the surface-bound and free styrene products, respectively. The free and surface-bound benzyl radicals continue the chain by abstracting a hydrogen atom from ~~DPP (**3**) to form the free and surface-attached toluene (eq 11) while regenerating **13** and **14**. Since at these low conversions the two product pairs, **4** + **5** and **6** + **7**, are formed in essentially equal amounts, it appears that radicals **13** and **14** are formed with nearly equal probability and their β-scission reactions occur efficiently. As shown below, this lack of regioselectivity in cracking at low conversions is not the case at higher conversions or at low initial ~~DPP surface coverages.

Occasionally the radical chain process terminates through benzyl radical coupling. In the fluid-phase studies, chain termination was also found to occur by benzyl radical coupling and was shown to result from the fact that $k_5 \gg k_4[1]$ and, hence, $[PhCH_2^{\bullet}] \gg [PhCHCH_2CH_2Ph]$ to maintain equal rates for steps 4 and 5 at steady state.[18] In the surface case, there are three possible benzyl radical termination products: $Ph(CH_2)_2Ph$ (**10**), ~~$Ph(CH_2)_2Ph$ (**15**), and ~~$Ph(CH_2)_2Ph$~~ (**16**). The doubly attached product **16** is not detected among the reaction products, and this may be a consequence of inhibited diffusion of surface-bound radicals as observed previously.[16] Conformational strain effects may also hinder the formation of such a doubly attached species with only two methylene units in the bridge. As indicated by the formation of product **11** (see below), however, it is feasible to generate a corresponding species on the surface if there are three methylene units in the bridge. Termination product **10** is detected in the product mix while the detection of **15** is obscured by a trace impurity in the sample that elutes at the same GC retention time.

The kinetic chain length for the radical chain process on the surface could be calculated from the amount of **10** formed (plus **15** if present) or from the amount of PhC_2H_5 (**8**) generated in step 10. The very small amounts of these products formed make quantitation quite difficult in the cases where they are detected. However, a useful semiquantitative estimate of the combined chain length for the two parallel radical chains can be made on the basis of [(**5**) + (**7**)]/4(**8**) assuming no selectivity in eq 9 and that all radicals produced initiate chains, or from [(**5**) + (**7**)]/2(**10**) assuming bibenzyl is the only significant chain termination product. These calculations give estimates of 250–500 for the chain length, indicating that the radical chain induced decomposition process remains very efficient under surface-immobilized conditions at high coverage (in the liquid phase, only a lower limit of 100 could be placed on the kinetic chain length[18]).

As the conversion of ~~DPP increases, there is a divergence in the yields of the four main products, and several secondary products are formed in small but increasing amounts as shown in Figure 1. The most significant of these (reaching only about 2.8 mol % at 23% conversion) is ~~$Ph(CH_2)_3Ph$~~ (**11**), which was identified as 1,3-bis(*p*-hydroxyphenyl)propane or the corresponding bis(trimethylsilyl ether) derivative after workup. The formation of this doubly attached product arises from a secondary reaction that consumes surface-bound styrene (**5**) probably by addition of a surface-bound benzyl radical (which would normally have reacted to form **6**) to **5**. Other secondary products include the two possible doubly attached 1,3,5-triphenylpentane isomers, ~~$PhCH(CH_2CH_2Ph$~~)CH_2CH_2Ph and ~~$PhCH_2CH_2CH(CH_2CH_2Ph$~~)Ph, that presumably were formed from addition of radicals **13** and **14** to **5** and have their analogue, 1,3,5-triphenylpentane, among the secondary products detected in the thermolysis of liquid-phase DPP.[18] Several other isomers corresponding to the same composition, ~~$C_{23}H_{22}$~~, are also detected but have not been identified. The amounts of all these isomers have been combined and listed in Table I as **12** and reach a maximum of 1.8 mol % at 23% ~~DPP conversion. Formation of **12** and **11** highlight the fact that cracking reactions such as eq 1 are only slightly preferred thermodynamically over the reverse addition at these temperatures. In fact, the equilibrium constant for eq 1 has been calculated by thermochemical methods to be only ca. 41 atm ($\Delta G° = -4.7$ kcal/mol) at 365 °C, which corresponds to $K_c = 0.8$ M.[18] The final secondary product observed is ~~PhC_2H_5 resulting from the hydrogenation of **5** (only trace amounts are produced from steps 9a plus 10). Alkenes such as styrene and stilbene are known to be reduced to the alkanes in the presence of hydrogen donors such as tetralin[6,7b,21b] as well as by DPP itself.[18] The lack of secondary products from vapor-phase styrene in the present experiments is a consequence of the experimental design, in which vapor-phase products migrate out of the heated zone into the cold trap as they are formed.

It is possible to perform an internal stoichiometric balance since amounts of products from vapor-phase C_7 fragments must be equal to amounts of products from surface-attached C_8 fragments, and products from vapor-phase C_8 fragments must equal those from surface-attached C_7 fragments. The (free C_7)/(surface C_8) ratio is defined as (**4**)/[(**5**) + (**9**) + (**11**) + (**12**)] with all isomers of **12** assumed to result from secondary reactions of **5**. The (free C_8)/(surface C_7) ratio is defined as (**7**)/[(**6**) + (**11**)]. Both ratios, which are calculated in Table I, are close to the ideal value of unity, with each giving an average value for the 15 runs at high coverage of 1.00 ± 0.06. This result gives added confidence to the internal consistency of the quantitation and added confidence that no significant products are undetected.

The data in Figure 1 also show that as the conversion of ~~DPP increases, an increasing selectivity develops for the radical chain path that forms **6** and **7** relative to that which forms **4** and **5**. This accumulating selectivity is most accurately portrayed by the styrene (**7**) to toluene (**4**) ratio, which is calculated in Table I and plotted as a function of conversion in Figure 2, since these products are not consumed in secondary reactions. Data for both batches of high-coverage material are plotted together but identified separately. As seen in Figure 2, the (**7**)/(**4**) ratio increases monotonically with conversion from values of 1.00 ± 0.02 at conversions <4% to a value of 1.41 ± 0.04 at 23% conversion. A linear regression of the data gives a slope of 0.021 ± 0.001 and an intercept at 0 conversion of 0.95 ± 0.02 ($r^2 = 0.981$). The present data do not allow a determination of whether the regression line is actually curved at very low conversions to give a limiting value near 1 (no selectivity), or if the extrapolated value of 0.95 at 0 conversion is meaningful. Recent data from studies of the thermolysis of fluid-phase *p*-$(CH_3)_3SiOC_6H_4(CH_2)_3Ph$, which can be used to model the influence of a *p*-silyloxy substituent on the regioselectivity of thermal cracking in ~~DPP, did give a corresponding value of 0.91 ± 0.02 at 375 °C for this measure of selectivity.[23] This value indicates that there is a slight inherent selectivity for the formation of the benzylic radical that is para to the silyloxy substituent.[25] In the thermolysis of ~~DPP, the important result from Figure 2 is that as the conversion

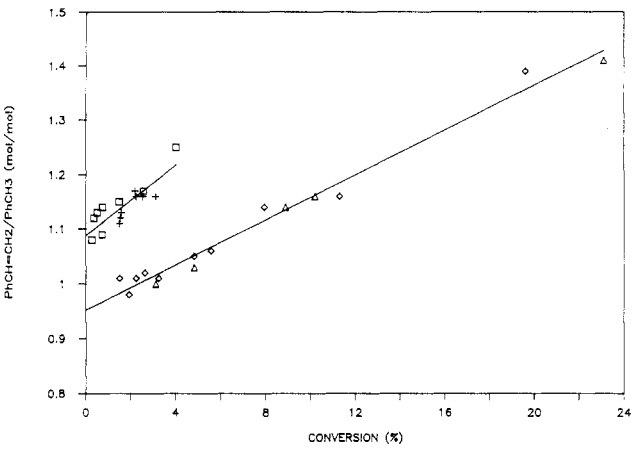

Figure 2. Regioselectivity in the thermolysis of ~~DPP as a function of conversion level and surface coverage: □, 0.132 mmol g^{-1}; +, 0.142 mmol g^{-1}; ◇, 0.566 mmol g^{-1}; △, 0.586 mmol g^{-1}.

increases, there is an *increasing selectivity in the opposite sense*, which favors the formation of **6** and **7**.

The explanation for this unusual regioselectivity as conversion increases appears to lie in the hydrogen transfer propagation step 11, which generates the benzylic radicals **13** and **14** that undergo the facile unimolecular β-scission steps 12 and 13. Enhanced formation of radical **14** relative to **13** in step 11 leads to enhanced selectivity for the formation of product pair **6** and **7**, as observed. As conversion increases, ~~DPP molecules become increasingly distant from hydrogen abstracting benzyl radicals that remain attached to the surface, and they are also separated by increasing quantities of surface-bound product molecules such as **5** and **6**. The combination of these effects apparently leads to a higher probability for hydrogen abstraction at the benzylic carbon that is farthest from the surface as illustrated below.

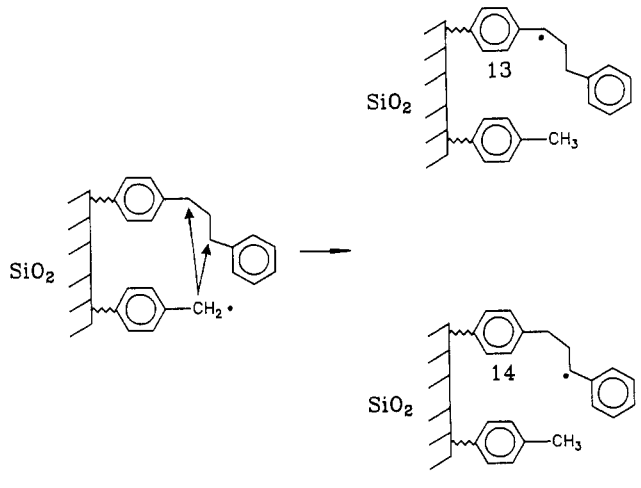

It should be noted that a hydrogen exchange reaction between a molecule of ~~$PhCH_3$ product and ~~$PhCH_2$•, although chemically unproductive, does provide a chemical means for migration of the radical center on the surface, while perhaps bringing the radical in closer proximity to an unreacted ~~DPP molecule. On the other hand, ~~$PhCH_3$ and other product molecules could potentially act as physical barriers to the hydrogen transfer in such a way that there is again a higher probability for a radical to abstract the benzylic hydrogen of ~~DPP that is farthest from the surface. This hypothesis gains some support from the results of studies at low initial surface coverage discussed below.

Two batches with lower initial surface coverages of ~~DPP of 0.142 and 0.132 mmol g^{-1} were prepared, and thermolysis studies were conducted at 345–375 °C for ~~DPP conversions of 0.3–3.9%. The reaction rate, which will be elaborated upon in the text section, is substantially depressed at these lower coverages, and only a 3.9% conversion of ~~DPP is obtained after 8 h at 375 °C. The product data are presented in Table II. The reactions are quite clean, and the material and internal stoichiometric balances are good, although more scatter in the data is observed because of the extremely small quantities of products being analyzed. The (free C_7)/(surface C_8) ratio gives an average value of 0.93 ± 0.07 for the 15 runs with the two batches, while the corresponding average value for the (surface C_7)/(free C_8) ratio is 0.98 ± 0.06.

A significant feature of the data in Table II is the observation of the selectivity for formation of the product pair **6** and **7**, but at much lower conversions and in the absence of any secondary products. The values for the (**7**)/(**4**) ratio, used as a measure of the cumulative selectivity, are given in Table II and plotted as a function of ~~DPP conversion in Figure 2 along with the corresponding high-coverage results. Linear regression of the low-coverage data gives a slope of 0.032 ± 0.005 and intercept at 0 conversion of 1.09 ± 0.02 (r^2 = 0.746). It is clear that measurable selectivities are detected at very low conversions, again showing a preference for hydrogen abstraction to form **14** over **13** and resulting from surface DPP molecules being more remote from hydrogen abstracting radicals. It is interesting to note that although the initial surface coverage has been reduced by a factor of about 4, the regioselectivity is less than that measured for high-coverage ~~DPP at only 23% conversion. This observation suggests that the presence of moderate quantities of product molecules on the surface may contribute to the regioselectivity by acting as physical barriers which impede hydrogen transfer propagation step 11a more than 11b. We are in the process of testing this hypothesis through studies in which an inert aromatic molecule is coattached to the surface with DPP molecules to act as a physical spacer.

Reaction Rate. One of the important implications for low-temperature coal thermolysis derived from earlier studies of fluid-phase DPP was that trimethylene (and longer) links between aromatic moieties are readily cracked at significant rates at 375–400 °C, contrary to thermochemical predictions of stability based solely on rate-controlling C–C bond homolysis. This result was readily explained experimentally and on thermochemical grounds by the radical chain induced decomposition pathway described by eq 2–6.[18] As shown above, a simple analysis of initial rate of conversion of surface-immobilized DPP at saturation coverage indicates that it is decaying at a rate comparable to that of liquid-phase DPP, and hence, to a first approximation, the rate of the radical chain process is not substantially affected by surface immobilization. We shall now examine the rate behavior in more detail, including its dependence on surface coverage.

(25) Substituent effects are expected to be small in these hydrogen atom transfer reactions involving nonpolar radicals.[26]

(26) Russell, G. A. In *Free Radicals*; Kochi, J. K., Ed.; Wiley: New York, 1973; Vol. 1, Chapter 7.

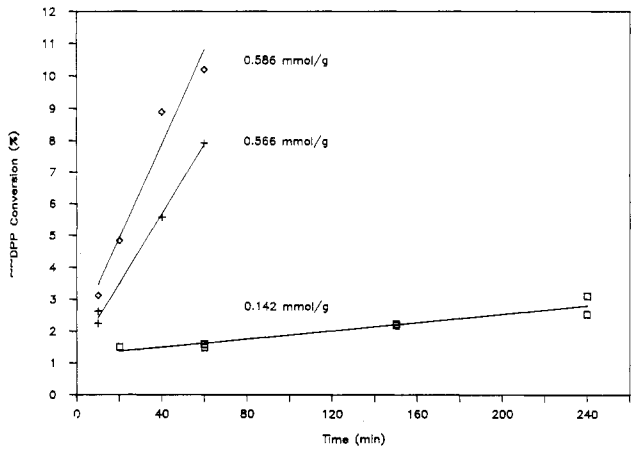

Figure 3. Rate of conversion of ~~DPP as a function of surface coverage at 375 °C: ◇, 0.586 mmol g^{-1}; +, 0.566 mmol g^{-1}; □, 0.142 mmol g^{-1}.

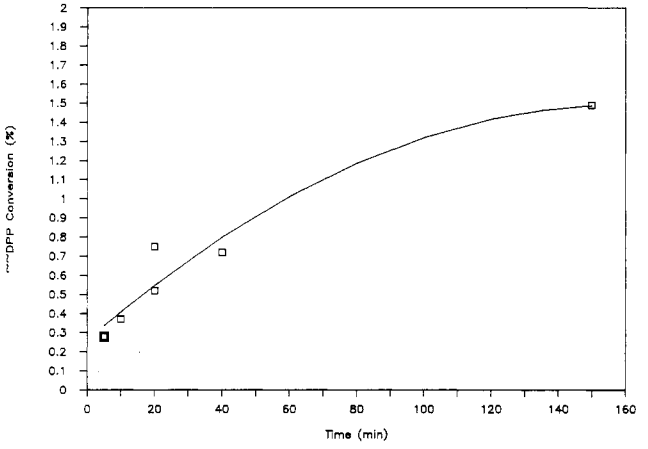

Figure 4. Rate of conversion of ~~DPP at 345 °C and surface coverage of 0.132 mmol g^{-1}.

The rate of ~~DPP conversion at 375 °C is shown in Figure 3 for the batches with coverages of 0.586, 0.566, and 0.142 mmol g^{-1}. The plots are shown for low ~~DPP conversions of ≤10% where they should show negligible curvature regardless of the exact kinetic order. Unexpectedly, the linear regression lines, which fit the data well (see below), extrapolate to positive conversions at 0 time, suggestive that there is a faster rate component for the very early stages of the reaction. This feature is most clearly seen in Figure 4 with data obtained on the 0.132 mmol g^{-1} batch, where studies at the lower temperature of 345 °C begin to show the curvature and fast initial rate component at very low conversions. Experiments indicate that this fast initial rate is not a result of the standard sample handling procedures (see Experimental Section). Instead of employing a full degassing procedure, one sample was heated at 345 °C for 20 min after evacuation for only 1 h to a final pressure of 5×10^{-5} Torr instead of for 18 h to a final pressure of 2×10^{-6} Torr. The measured ~~DPP conversion of 0.6% was not significantly different from that shown in Figure 4 for a corresponding run employing the normal procedure. Secondly, a reaction was performed with the normal handling procedure for the 20-min period at 345 °C giving the anticipated ~~DPP conversion of 0.5%. The reaction residue was then transferred to a new reaction tube, degassed and sealed off in the standard manner, and reacted for an additional 20 min. The incremental ~~DPP conversion obtained was only 0.17% (total conversion of 0.67%), a value consistent with that for a typical 40-min run (0.7% conversion, Table II). Hence, it appears that the reason for the accelerated rate at very early conversions is indigenous to the surface-immobilized material rather than its gas-phase surroundings. It is not known if the rate irregularity is the result of a trace amount of impurity on the surface acting as initiator for this long chain free-radical process or some currently unexplained fundamental aspect of the reaction. As described above, the reaction rate for ~~DPP thermolysis can be accelerated by the presence of a free-radical initiator. Whatever the cause of the initial rate disturbance in the thermolysis of ~~DPP, it appears to affect only the very earliest stage of the reaction and is substantially over by about 1% conversion.

In the following discussion, we will take the slopes of the linear regression lines of Figure 3 as being characteristic of the initial rate of ~~DPP thermolysis following the brief initial rate disturbance. The linear regressions of the data at 0.586, 0.566, and 0.142 mmol g^{-1} give the following slopes as initial rates (in units of % ~~DPP conversion per hour) at 375 °C, respectively: 8.9 ± 1.5 (r^2 = 0.954), 6.6 ± 0.3 (r^2 = 0.996), and 0.39 ± 0.05 (r^2 = 0.912). The two high-coverage batches show fair agreement between their measured initial rates. For the sake of comparison of these rates with the rate of decomposition of liquid DPP, we use the mutually consistent sets of Arrhenius parameters determined previously. Poutsma and co-workers[18] found log A = 13.1 $M^{-1/2}$ s^{-1} and E_a = 52.3 kcal mol^{-1} over the temperature range 343–425 °C, while Gilbert and co-workers[19a,27] found log A = 12.5 $M^{-1/2}$ s^{-1} and E_a = 51.4 kcal mol^{-1} over the temperature range 335–380 °C for the nominally $^3/_2$-order reaction in DPP (n = 1.59,[18] 1.55[19a]). At 375 °C, the resulting rate constants are calculated to be $k = 2.88 \times 10^{-5}$ $M^{-1/2}$ s^{-1} [18]and $k = 1.46 \times 10^{-5}$ $M^{-1/2}$ s^{-1}.[19a] Employing estimates of vapor pressures and densities of DPP,[18] one calculates estimated initial rates of liquid DPP conversion at 375 °C of 18 and 9% h^{-1} employing the two rate constants.[28] Hence the measured initial rates for reaction of ~~DPP *at high coverage*, 7–9% h^{-1}, are comparable to those reported for liquid DPP. Although this agreement in rates may be fortuitous, the comparison serves to illustrate the fact that the radical chain decay of DPP occurs readily at high coverages even under conditions of restricted mobility.

However, as shown in Figure 3, a substantial rate depression is observed upon lowering of the surface coverage of ~~DPP to 0.142 mmol g^{-1}. The rate depression for this 4-fold decrease in surface coverage is a factor of 17–23 compared with the two high-coverage batches. This rate decrease is substantially larger than the factor of $4^{3/2}$ = 8 calculated for the rate decrease resulting from a 4-fold decrease in concentration of fluid-phase DPP, whose thermolysis is $^3/_2$ order in DPP concentration. It appears that the thermolysis rate for DPP attached to the surface is more sensitive to the global surface coverage than the rate of fluid-phase DPP is to concentration. This presumably reflects a substantial sensitivity for the rates of bimolecular reaction steps 10 and 11 to the proximity of surface DPP molecules and hydrogen abstracting radicals, particularly those that are also surface attached. As dis-

(27) The units for log A in ref 19a were given, presumably mistakenly, in s^{-1}.

(28) Preliminary studies of the thermolysis of p-$(CH_3)_3SiOC_6H_4$-$(CH_2)_3Ph$ indicate that the p-silyloxy substituent has only a small rate-enhancing effect (ca. 1.2-fold at 375 °C) on the thermolysis of the DPP moiety in fluid phases.[23]

cussed previously,[16a] the situation on the surface is complicated by the fact that it is not clear how to define rate constants and "concentration" for bimolecular reaction steps such as eq 10 and 11 when the reacting species are surface attached. Since the molecules are not free to diffuse, the kinetic driving force for such reaction steps depends in some inverse fashion on the distance between reacting sites weighted by the conformational mobility of each surface-attached reacting species. Additional research is in progress to shed light on this issue.

Implications for the Thermal Chemistry of Coal. These studies have shown that the facile radical chain induced decomposition reaction discovered for fluid-phase DPP still occurs at a comparable rate under conditions of surface immobilization. Hence structural units in coal such as $Ar(CH_2)_nAr'$ with $n \geq 3$ (or similar structural fragments as part of some appropriately substituted hydroaromatic) possess linkages that can be cracked at modest temperatures by radical chain processes involving β-scission of benzylic radicals. The rate of ~~DPP thermolysis by this radical chain induced decomposition pathway is highly sensitive to surface coverage and the proximity of hydrogen abstracting radicals to the benzylic methylene hydrogens of ~~DPP. When such linkages between aromatic clusters are present in the coal macromolecular framework and are somewhat isolated from other hdyrogen abstracting radicals generated in the network, the presence of mobile radical sources (such as vapor-phase or solvent-derived in the case of coal liquefaction) will be beneficial for their efficient degradation.

It is also significant that restricted diffusion can also alter expected product distributions. Even at these elevated temperatures, regiospecific hydrogen transfer reactions can be detected that proceed contrary to expectations based on electronic considerations, and that result solely from restricted radical and substrate mobility. This is illustrated in the present study of ~~DPP thermolysis where formation of ~~$PhCH_2CH_2\dot{C}HPh$ (**14**) over ~~$Ph\dot{C}HCH_2CH_2Ph$ (**13**) is increasingly preferred as the distance between DPP moieties and radical centers on the surface increases and has stoichiometric consequences for product yields.

Experimental Section

GC analyses were performed on a Hewlett-Packard 5880A gas chromatograph employing a J & W Scientific 30 m × 0.25 mm i.d. DB-1 bonded-phase methylsilicone capillary column and flame-ionization detection. Detector responses were calibrated with the use of experimentally determined response factors in all cases where authentic samples were available (see below) or with estimated response factors based on carbon numbers. Mass spectra were obtained at 70 eV with a Hewlett-Packard 5995A gas chromatograph–mass spectrometer equipped with a capillary column matched to that used for GC analyses.

Synthesis of p-$HOC_6H_4(CH_2)_3Ph$ (17). p-Cinnamylphenol was prepared according to the procedure of Jurd by the alkylation of phenol with cinnamyl alcohol in aqueous citric acid/ascorbic acid.[29] The resulting olefin was hydrogenated for 18 h in ethyl acetate by using 10% Pd/C catalyst and 35 psig of hydrogen pressure. Following removal of catalyst and solvent, the crude product was recrystallized three times from hexanes to give p-(3-phenylpropyl)phenol (**17**) that was 99.9% pure by GC: mp 62–63 °C (lit.[29b] mp 63–64 °C); mass spectrum, m/z (relative intensity) 212 (M^+, 57), 121 (19), 120 (14), 108 (20), 107 ($HOC_6H_4CH_2^+$, 100), 92 (31), 91 (36), 77 (43), 65 (15); after trimethylsilylation 284 (M^+, 8), 180 (12), 179 (68), 92 (12), 91 (100), 77 (16), 73 (99), 65 (20).

Preparation of Surface-Attached 1,3-Diphenylpropane (3). Procedures for preparation, analysis, and thermolysis of surface-attached diphenylalkanes have been described in detail elsewhere,[16a] and only highlights will be given below. Phenol **17** was adsorbed onto the surface of a dried, fumed silica (Cabosil M-5, Cabot Corp., 200 ± 25 $m^2\ g^{-1}$, ca. 4.5 OH/nm^2) by solvent evaporation from a benzene slurry. The attachment reaction was performed at 225 °C for 1 h in a fluidized sand bath on a thoroughly degassed, evacuated (5×10^{-5} Torr), and sealed sample of the resulting solid. The sample was then transferred to another tube, connected to a vacuum at 5×10^{-3} Torr, and heated in a tube furnace at 270–300 °C to remove unreacted **17**. The lower temperature in this range appeared to lead to a product of slightly higher purity. For the two batches prepared at "saturation" coverages, excess (2–3-fold) **17** was employed relative to the surface hydroxyl population (mole basis), while lower surface coverages of **3** were prepared by limiting the amount of **17** used. The final product, which is a free-flowing white powder, was assayed by using a base hydrolysis procedure. Three replicate samples of **3** were each digested in 1 N NaOH, and p-$HOC_6H_4(CH_2)_2Ph$ was added as an internal standard. The mixtures were acidified, extracted with CH_2Cl_2, dried over sodium sulfate, and filtered, and the solvent was removed by evaporation. The residual phenols in the samples were then silylated with *N,O*-bis(trimethylsilyl)-trifluoroacetamide (BSTFA) in pyridine and the samples analyzed by GC. Surface coverages so determined were reproducible to at least ±2%.

Thermolysis Procedure. A weighed amount of **3** (0.3–0.6 g) was loaded into one end of a T-shaped Pyrex tube, degassed by repetitive evacuation and purging with argon, and sealed under vacuum (2×10^{-6} Torr). Thermolyses were performed in a horizontal temperature-controlled tube furnace fitted with an internal copper cylinder containing a center cylindrical hole just large enough to contain the sample tube and a thermocouple. The sample was placed in the preheated furnace (±1 °C), and volatile products migrated outside the heated zone into the vertical leg of the tube contained in a liquid nitrogen bath. At the end of the reaction, an acetone solution of these volatile products was analyzed by GC and GC–MS with m-xylene used as the GC internal standard. After evaporation of the acetone, the quantity of phenol **17** evolved into the trap was analyzed by GC following silylation employing p-$HOC_6H_4(CH_2)_2Ph$ as internal standard. The solid residue was analyzed for surface-attached products by digestion of the residue in aqueous base in an analogous procedure to the surface coverage assay procedure described above. 2,5-Dimethylphenol and p-$HOC_6H_4(CH_2)_2Ph$ were added as GC internal standards. In this residue analysis, care must be taken to quickly extract the phenolic mixture away from the aqueous phase following acidification since p-vinylphenol (corresponding to surface-attached product **5**) is unstable in the presence of acid. The resulting mixture of phenols was silylated and analyzed by GC and GC–MS. Analysis of the trimethylsilyl ether derivatives typically gave more reproducible quantitative results than analysis of the phenols directly. Benzyl phenyl ether used as a radical initiator in a few runs was kindly provided by B. M. Benjamin and was 99.2% pure by GC analysis.

Product Assignments. Samples of nonphenolic products **4**, **7**, **8**, and **10** were all commercially available, as were the phenols corresponding to the surface-attached products **6** and **9**. Product assignments were made on the basis of comparisons of mass spectra and GC retention times with these standard materials.

Identification of p-vinylphenol, corresponding to surface-attached product **5**, was based on mass spectra: m/z (relative intensity) 120 (M^+, 100), 119 (20), 91 (43), and 65 (15); after trimethylsilylation 192 (M^+, 100), 177 (84), 161 (17), 151 (20), 149 (14), 91 (11), 77 (17), 73 (22), and 65 (14).

1,3-Bis(p-hydroxyphenyl)propane, corresponding to **11**, was prepared in four steps by the procedure of Richardson and Reid.[30] Base-catalyzed condensation of p-methoxyacetophenone and p-anisaldehyde gave 1,3-bis(p-methoxyphenyl)-2-propen-1-one,

(29) (a) Jurd, L. *Tetrahedron Lett.* **1969**, 2863. (b) Jurd, L.; Stevens, K. L.; King, A. D.; Mihara, K. *J. Pharm. Sci.* **1971**, *60*, 1753.

(30) Richardson, E. M.; Reid, E. E. *J. Am. Chem. Soc.* **1940**, *62*, 413.

which was reduced in two steps by catalytic hydrogenation with 10% Pd/C in ethyl acetate followed by Clemmensen reduction. Demethylation with refluxing HBr/HOAc gave the final product, $HOC_6H_4(CH_2)_3C_6H_4OH$, in overall 65% yield. The product was recrystallized from CCl_4: mp 105–106 °C (lit.[30] mp 107–108 °C); mass spectrum, m/z (relative intensity) 228 (M^+, 24), 134 (21), 121 (37), 108 (33), 107 (100), 91 (12), 77 (44); after trimethylsilylation 372 (M^+, 29), 206 (18), 193 (18), 180 (22), 179 (76), 73 (100).

For the isomeric mixture of diphenols of composition $C_{23}H_{22}(OH)_2$, corresponding to **12**, two isomers comprising ca. 40% of the mixture were tentatively identified as 1,3-bis(*p*-hydroxyphenyl)-5-phenylpentane (**12a**), $HOC_6H_4CH(CH_2CH_2C_6H_4OH)CH_2CH_2Ph$, and 1,5-bis(*p*-hydroxyphenyl)-3-phenylpentane (**12b**), $HOC_6H_4CH_2CH_2CH(CH_2CH_2C_6H_4OH)Ph$, by comparison of GC retention times and mass spectra for their trimethylsilyl derivatives[31] (M_r = 476) with those for the same compounds produced directly from the thermolysis of p-$(CH_3)_3SiOC_6H_4(CH_2)_3Ph$.[23] The mass spectrum assigned to **12a** after trimethylsilylation is as follows: (relative intensity) 476 (M^+, 23), 283 (25), 180 (17), 179 (100), 117 (14), 91 (43), and 73 (81). The mass spectrum assigned to **12b** is as follows: 476 (M^+, 28), 193 (27), 180 (24), 179 (65), and 73 (100). The other four isomers (**12c–f**) (M_r = 332 as phenols; M_r = 476 when trimethylsilylated[31]) comprise 60% of the mixture. These unidentified isomers gave mass spectra with weak parent ions at m/z 476 (≤4%) and similar fragment ions at m/z 283, 193, 179, 91, and 73.

(31) Isomers **12a** and **12b** give resolved GC peaks in their bis(trimethylsilyl ether) form (M_r = 476), but are only partially resolved as phenols (M_r = 332). Isomers **12c–f** are well-resolved by GC from **12a,b**, but are again severely overlapped with each other in the underivatized phenol form.

Acknowledgment. Research was sponsored by the Division of Chemical Sciences, Office of Basic Energy Sciences, U.S. Department of Energy under contract DE-AC05-840R21400 with Martin Marietta Energy Systems, Inc. We appreciate many valuable discussions with Dr. M. L. Poutsma of ORNL.

Registry No. $Ph(CH_2)_3Ph$, 1081-75-0; p-$HOC_6H_4(CH_2)_3Ph$, 34591-21-4; *p*-cinnamylphenol, 24126-82-7.